Introduction

Unreinforced masonry (URM) was a common construction material used in New Zealand (NZ) from the 1880s-1930s. However, the popularity of URM construction declined following the 1931 Hawke's Bay earthquake, which destroyed a significant portion of the local URM building stock, as most URM buildings lacked the tensile resisting elements required to sustain seismic loads. URM construction was eventually either prohibited or rigorously restricted in most seismic zones following the establishment of the New Zealand Standard Building By-Law NZS 1900 in 1965 [1]. It is estimated that approximately 3500 URM buildings existed in NZ in 2010 [2], with these buildings comprising a significant portion of NZ's heritage building stock [3]. Consequently the preservation of these historic URM buildings is of paramount importance, with an improvement in their earthquake performance being a priority.

When subjected to seismic acceleration, an URM wall can fail in either the in-plane or out-of-plane direction, depending on the orientation of earthquake loading. While it is typically the in-plane wall characteristics that dictate the global structural integrity of an URM building, walls collapsing in the out-of-plane direction can cause a significant amount of damage, particularly to adjacent property. More importantly, out-of-plane URM wall failures represent a major hazard for nearby pedestrians during a design level earthquake. Due to the lack of tensile resisting elements, when loaded in the out-of-plane direction an URM wall derives resistance from only the wall axial load and selfweight counteracting the moments developed due to lateral loads. Many URM walls also fail in an out-of-plane manner due to connection failures between perpendicular walls and/or between walls and diaphragms, with wall

[1]Structural Engineer, EQ Struc Group, Auckland, New Zealand, ylin126@aucklanduni.ac.nz.
[2]General Manager, Reid Construction Systems, Auckland, New Zealand, dlawley@reids.co.nz
[3]EQC Research Fellow, Department of Civil and Environmental Engineering, University of Auckland, Private Bag 92019, Auckland, New Zealand, l.wotherspoon@auckland.ac.nz
[4]Professor, Department of Civil and Environmental Engineering, University of Auckland, Private Bag 92019, Auckland, New Zealand, j.ingham@auckland.ac.nz.

thickness, wall slenderness ratio, and wall-to-diaphragm connections having been identified as crucial parameters in determining wall out-of-plane capacity [4-7]. The vulnerability of URM walls loaded in the out-of-plane direction has been demonstrated in several recent NZ earthquakes, such as the M6.8 2007 Gisborne earthquake, the M7.1 2010 Darfield earthquake, and the M6.3 2011 Christchurch earthquake [8].

A variety of strengthening techniques exist to enhance the out-of-plane capacity of URM walls, typically involving the addition of tensile resisting elements to existing walls. Examples of common tensile resisting elements include Kevlar fabric and carbon tow sheets [9], carbon fibre reinforced polymer (CFRP) bars epoxied in a shallow slot cut in the wall using a technique termed Near Surface Mounting (NSM) [11], textile reinforced mortars (TRM) applied to wall surfaces [12], and shotcrete used to strengthen a multi-storey masonry building [13].

Engineered Cementitious Composite (ECC) is a cement composite that is reinforced with synthetic fibres. When loaded in tension, ECC exhibits a strain-hardening characteristic through the process of micro-cracking, with the crack widths being typically less than 100 μm [14]. ECC has been previously used as tensile reinforcement for URM wall panels [15], as partial tensile reinforcement for bridge slabs [16], and as tensile reinforcement for concrete beams [17], with a strength increase of 36-80% reported in the latter study when compared to the performance of equivalent unstrengthened beams. The objective of the study reported here was to investigate the effectiveness of ECC to enhance the out-of-plane capacity of URM walls, and this study was a companion to an investigation considering the use of ECC for in-plane URM wall strengthening [18]. Other investigations of ECC effectiveness in strengthening URM elements have been documented in [19-21].

Experimental program

Details of the ECC constituent materials and their proportions as used in this study are presented in Table 1, with the materials provided in a bagged form by the supplier. The design (lower 5% characteristic) tensile and compressive strengths of ECC were recommended by the supplier as 1.9 MPa and 40 MPa respectively and were adopted accordingly, with the mean tensile strength being 3.1 MPa.

Table 1: Mix proportions of the ECC used in testing

Material	Proportions (kg/m^3)
Sand	64
Portland cement	76
Calcium Aluminate (CA) cement	4
Fly ash	24
Water	37.4
Super Plasticiser	0.26
Stabiliser	0.041
Fibres	0.26

The aims of the study were to determine whether ECC shotcrete can enhance the out-of-plane moment capacity of URM walls, and whether a satisfactory design methodology can be established. Although in some cases it is possible to apply reinforcement to both wall surfaces, such as for internal partition walls, this type of configuration was not investigated and instead a constraint imposed in this study was to apply the seismic strengthening intervention to only a single surface of the wall such that when strengthening exterior URM walls, the application of ECC shotcrete is applied on the internal surface only and hence the external historic appearance of the building is preserved. Note that for all analyses conducted in this study it was assumed that the wall top and base are simply supported with the wall base rocking about its edge, and that connection failures will not occur. In practise such boundary connections can be easily achieved with appropriate wall-to-diaphragm anchorages. It is also important to note that due to the assumption of wall to diaphragm anchorages being present, it is expected that the diaphragm forces are transmitted to the stiff in-plane walls and does not exert additional demands to walls loaded in their out-of-plane direction. In practice such assumptions should be carefully evaluated as unrestrained diaphragms can exert significant thrust force to out-of-plane walls.

Test specimens

Five masonry walls measuring approximately 4.1 m high × 1.15 m long × 230 mm thick were constructed with a slenderness ratio (wall height to wall thickness) of 17.9. The nominated wall dimensions are similar to those adopted in [22-28]. Figure 1 shows construction of the first two walls, with the professional mason that constructed the wall specimens reported in [22-24, 26] also used in this study to ensure consistent workmanship between the comparable studies. The average compressive strengths of the clay bricks (f_b'), mortar (f_j') and masonry (f_m') as reported in Table 2 were determined using [29-31] respectively. The Common bond pattern with a header course located every four to six stretcher courses was adopted, as this is the predominant bond pattern observed in the NZ URM building stock [32].

Figure 1: Construction of clay brick unreinforced masonry walls

Table 2: Masonry constituent compressive strengths

	Material properties	
	Mean (N/mm^2)	Coefficient of variance (%)
Brick compressive strength (f'_b)	21.4	11
Mortar compressive strength (f'_j)	0.9	11
Masonry compressive strength (f'_m)	6.0	24

The full test configuration is shown in Table 3 and the wall configurations are designated as WX-SY-Z-N, where:

- X represents the wall number tested, ranging between 1 and 5 (wall 1 was tested twice, first as-built and then repaired with 30 mm of ECC on a single surface).

- Y represents the total thickness in mm of ECC shotcrete applied to the wall on a single surface.
- Z is either M or C depending on whether the wall was loaded monotonically (M) or cyclically (C).
- N refers to any additional notes that are explained in Table 3.

Table 3: Full out-of-plane wall test configurations

Wall designation	Thickness of ECC overlay (mm)
W1-S0-M	0
W1-S30-M-CL[1]	30
W2-S0-M	0
W3-S30-M-TL	30
W4-S25-C	25
W5-S30-C-NSM	30

Where: M = monotonically loaded, C = cyclically loaded
CL = ECC overlay on compression surface of loading
TL = ECC overlay on tensile surface of loading
NSM = Near Surface Mounted reinforcement used
[1]Wall 1 repaired with 30 mm of ECC on a single surface

An example of the wall designation is W3-S30-M-TL, representing wall number 3 with 30 mm of ECC shotcrete, that was loaded monotonically with the ECC located on the wall tensile surface.

Two types of strengthening configurations were investigated in this study. The first configuration entailed 25-30 mm of ECC shotcrete being applied to a single surface of the masonry walls, as in configurations W1-S30-M-CL, W3-S30-M-TL and W4-S25-C. The second configuration, shown in Figure 4, entailed a groove cut into the masonry wall surface and a grade 300 MPa D20 deformed reinforcing bar inserted 50 mm beneath the brick wall surface. The groove was later filled with ECC shotcrete and an additional 30 mm of ECC shotcrete was sprayed over the wall surface on the same side.

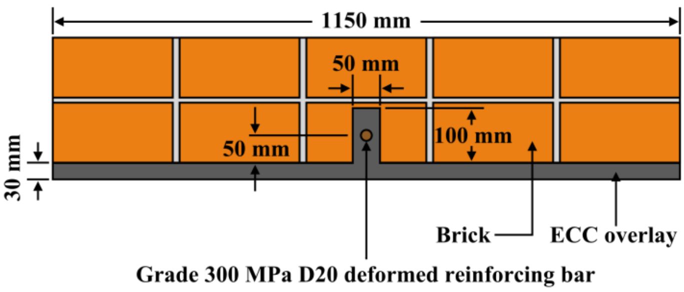

Figure 2: Cross-sectional view of the wall with near surface mounted reinforcing bar configuration (W5-S30-C-NSM)

Test setup

The test setup schematic is shown in Figure 3a and the actual test setup is shown in Figure 3b, with two steel rectangular hollow section reaction frames placed either side of the wall. Two sets of steel angles horizontally restrained both the wall top and wall bottom to provide pinned supports, with one set of angles connected to the strong floor and the other set of angles connected to the frame attached to the strong wall. This type of support condition is expected in URM buildings as the floor diaphragms are typically flexible and provide little restraint against potential wall rotation. A plywood frame was connected to the reaction frame (either frame depending on the direction of loading) through four S-shaped load cells that had an individual load capacity of 20 kN each. A set of two smooth steel plates with grease sandwiched between them provided the vertical support for the plywood frame. No other connections existed between the plywood and steel frame. Two air bags were inserted between the plywood frame and the masonry wall and were inflated using an air pump to provide a uniformly distributed horizontal pressure simulating seismic lateral inertial forces, similar to the loading scheme recommended by [33]. A linear variable displacement transducer (LVDT) or string gauge with a maximum horizontal extension of 500 mm was connected to the wall at mid-height to measure the mid-wall horizontal displacement, and data from the displacement gauges and load cells were collected at 50 Hz using a National Instruments data acquisition system. No axial overburden loads were applied to any of the walls, representing either a one-storey URM wall or the top storey of a two storey URM building. A similar test setup has been used to test URM walls of a comparable height to those investigated in this study and having a variety of thicknesses and axial load levels [22]. Studies reported in [24-26] employed this test setup to investigate the effectiveness of using near surface mounted (NSM) carbon fibre reinforced polymer (CFRP) strips and post-tensioned steel reinforcement to enhance the moment capacity of URM walls. The test setup has also been used in field testing conditions for the in-situ testing of URM partition walls [27-28].

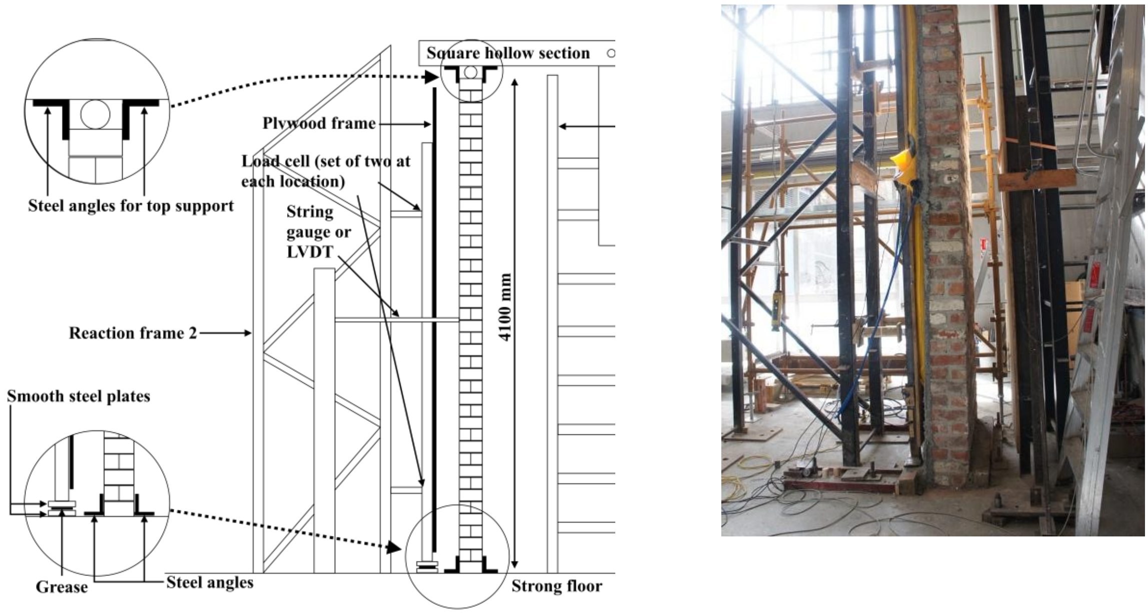

(a) Schematic drawing (b) Actual setup

Figure 3: Out-of-plane wall test setup

Implementation Procedure

After each wall was constructed, the mortar was air cured for 28 days and then ECC shotcrete was sprayed onto those walls that were to be strengthened. Prior to spraying, the wall surfaces were water blasted to both remove loose material and to pre-wet the surface. Timber planks were then attached to the sides of the walls to serve as an indicator of the thickness of ECC that needed to be sprayed. The ECC shotcrete was supplied in bagged form and was added to a two stage commercial shotcrete mixer from which the mixed material was pumped through a hose and sprayed onto the masonry walls. An interval of approximately 45 minutes was provided between the application of each successive 10 mm thick ECC layer, allowing the previously applied 10 mm layer to harden. Each sprayed layer was trowelled flat so that the next layer of ECC was applied onto a flat surface. Once spraying had been completed, the timber planks were removed and a constant water mist was applied onto the ECC shotcrete for 28 days.

It should be noted that due to the occasional unavailability of professional shotcrete applicators, the ECC overlays on wall W4-S25-C and W5-S30-C-NSM were sprayed by amateur applicators while all other walls were strengthened by professional shotcrete applicators. To account for the influence of applicator skill, a skill based strength reduction factor (ϕ_s) of 0.75 was applied when predicting the strengths of retrofitted walls that had received amateur ECC shotcrete application. This value of strength reduction factor was based on the results from a companion study [34] that investigated differences between the in-plane response of ECC reinforced concrete masonry wallettes prepared by either professional or amateur shotcrete applicators, where the amateur applicator strengthened wallettes had up to 25% reduction of in-plane strength when compared to the professional applicator strengthened wallettes.

Results

As-built wall

Loading was applied to the as-built walls until a clearly visible horizontal flexural crack developed, which for W1-S0-M occurred at the masonry bed joint at a 3.1 m height (75% of the wall height), with a maximum horizontal force of 4.2 kN and a corresponding out-of-plane wall displacement (measured at the crack location) of 2.6 mm. The wall was then further displaced to 115 mm (see Figure 4a). When the pressure inside the air bag was released, the wall returned to its original position and the crack closed up and was no longer visible. The reason why W1-S0-M did not crack near wall mid-height was attributed to the combined effect of flexural and axial stresses, where the axial compressive stress increases down the height of the wall due to self-weight distribution. This load combination results in the maximum flexural tension stress occurring above the wall mid-height, with the expected crack location being dependent on any overburden (in this case not present) and the mortar flexural tension strength, plus wall thickness and the effect of any mortar pointing [34]. For W2-S0-M, the principal horizontal flexural crack occurred 1.9 m above the ground, at approximately wall mid-height. The maximum force recorded was 4.5 kN, which was similar to the value obtained for W1-S0-M, after which the wall was further displaced to 18 mm laterally (see Figure 4b). W2-S0-M was not displaced beyond 18 mm because prior to testing the wall was already leaning in one direction as a result of the poor workmanship of the mason and hence it was suspected that displacing the wall to similar displacements as measured during testing of W1-S0-M could cause the wall to collapse under its own selfweight. The maximum lateral force resisted by the two as-built walls was approximately equal to the force generated by an earthquake with a peak ground acceleration of 0.23g. The force-displacement responses for the unstrengthened walls are summarised in Figure 4a and 7b, and show similar characteristics to those previously reported in [22].

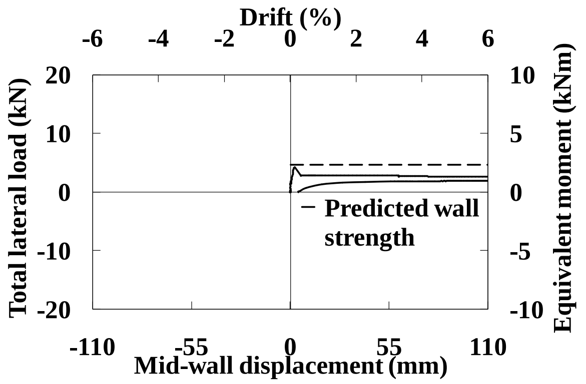

(a) As-built wall W1-S0-M

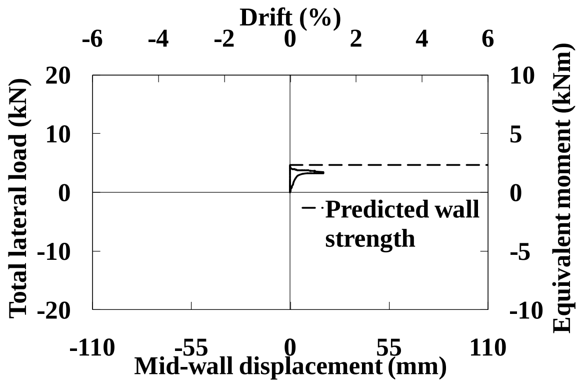

(b) As-built wall W2-S0-M

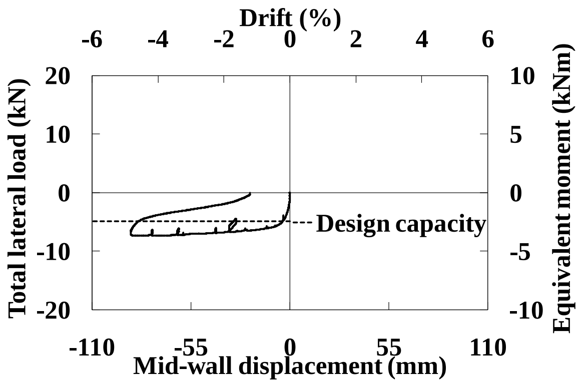

(c) Wall W1-S30-M-CL loaded monotonically with 30 mm ECC overlay on compression surface (Ideal capacity not shown due to value being similar to design capacity)

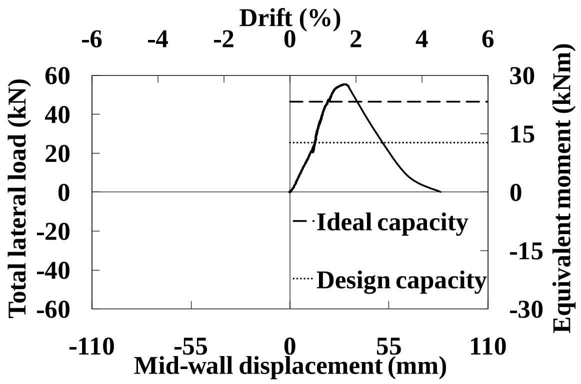

(d) Wall W3-S30-M-TL loaded monotonically with 30 mm ECC overlay on tensile surface

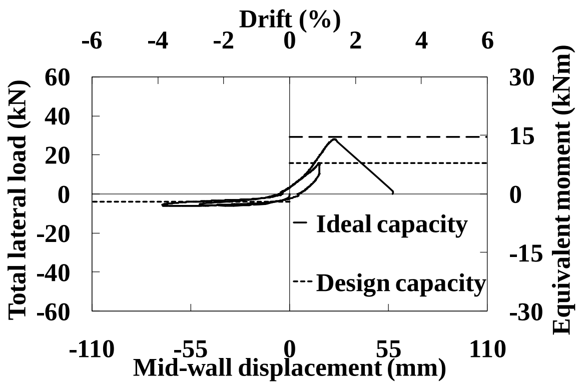

(e) Wall W4-S25-C loaded cyclically with 25 mm ECC overlay on a single surface (Ideal capacity on compression surface not shown due to similar value with design capacity)

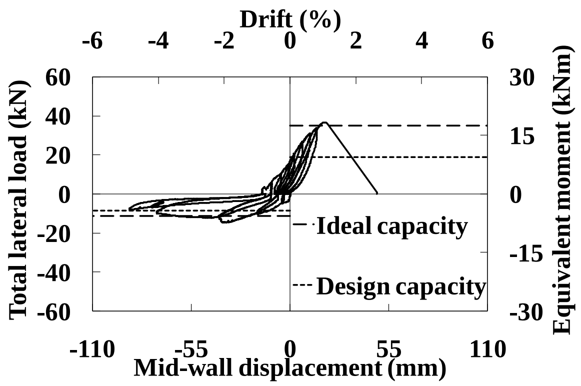

(f) Wall W5-S30-C-NSM loaded cyclically with 30 mm ECC overlay on a single surface and near surface mounted steel reinforcement

Figure 4: Out-of-plane wall responses

The cracking force per unit height and unit length of the wall was calculated using Equation 1 provided in [35], with the equation simplified due to the absence of an overburden force. w_{cr} is the wall cracking force per unit height and unit length of the wall, f'_{fb} is the masonry flexural bond strength, defined in [35] as 0.2 MPa for the two as-built walls constructed in this study, m_0 is the unit mass per unit area of wall, g is gravitational acceleration, equal to 9.81 ms^{-2}, and h and t are the height and thickness of the wall in mm respectively.

$$w_{cr} = \frac{f'_{fb} + 0.5 m_0 g \frac{h}{t} + \sqrt{f'_{fb}\left(f'_{fb} + m_0 g \frac{h}{t}\right)}}{1.5\left(\frac{h}{t}\right)^2} \tag{1}$$

Multiplying Equation 1 by the wall height and wall length results in a cracking strength of 4.7 kN, such that both measured loads were within 11% of the predicted strength, indicating good accuracy of the equation. Table 4 provides the maximum lateral forces recorded for both as-built and retrofitted walls.

Table 4: Out-of-plane wall test results

Wall designation	Measured lateral load (kN)	Wall crack height / wall height (β)	Predicted lateral load (kN)		Measured / predicted (%)	
			Design	Ideal	Design	Ideal
W1-S0-M	4.5	75%	4.7	N/A	96	N/A
W2-S0-M	4.2	46%	4.7	N/A	89	N/A
W1-S30-M-CL	7.4	46%	4.9	6.0	151	123
W3-S30-M-TL	55.1	50%	25.3	46.6	218	118
W4-S25-C	6.2[a], 28.1[b]	45%	3.9[a], 15.9[b]	4.5[a], 29.2[b]	159[a], 177[b]	138[a],96[b]
W5-S30-C-NSM	14.6[a], 36.6[b]	76%	8.5[a], 19.0[b]	11.2[a], 35.0[b]	172[a], 193[b]	130[a],105[b]

For the cyclic tests, a = loaded with ECC overlay on the compression surface, b = loaded with ECC overlay on the tensile surface

Strengthened walls

Wall W1-S30-M-CL had 30 mm of ECC shotcrete applied onto the compression surface of the wall and was loaded monotonically. The wall exhibited ductile behaviour with the ECC overlay behaving similarly to a steel plate in bending (see Figure 5). When the first cracking strength of the ECC overlay was reached, the wall continued to resist further load with increasing displacement as shown on the force-displacement graph in Figure 4c. The exposed brick wall surface had several wide flexural cracks (see Figure 6) but the bricks did not detach from the ECC overlay.

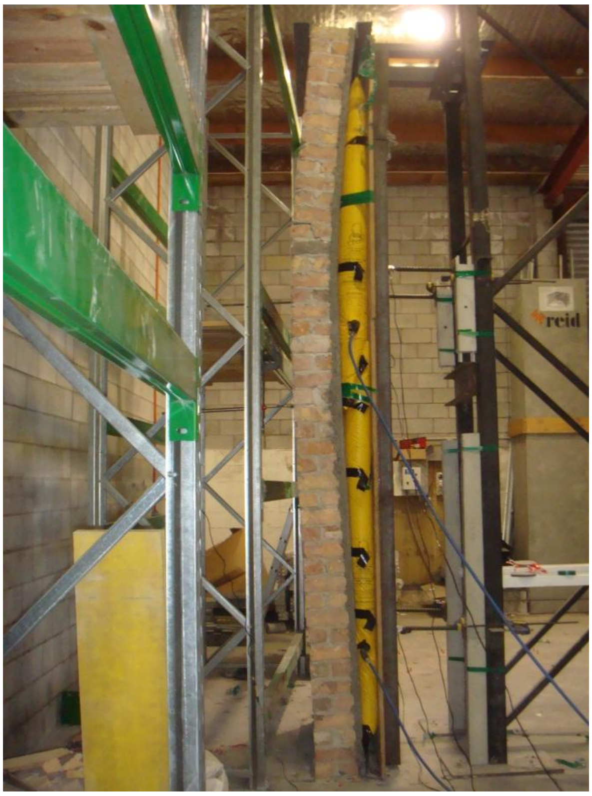

Figure 5: Ductile response exhibited by the wall when ECC was applied to the compression surface

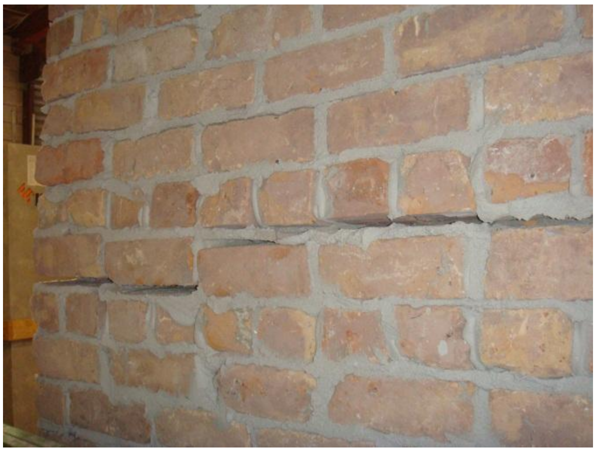

Figure 6: View of the major flexural crack observed on specimen W1-S30-M-CL

The total resistance against lateral forces of W1-S30-M-CL was calculated using Equation 2, which is equal to the lateral force required to overcome the moment capacity of the ECC overlay section, F_{ECC} (calculated using Equation 3) and F_{RM}, the lateral force required to overcome the restoring moment of the cracked wall due to wall selfweight per unit length of the wall. F_{RM} is calculated using Equations 4-6 and for Equation 3, f'_{yECC} is the tensile strength of ECC and Z is the section modulus of the ECC overlay section. Two predicted moment capacities were determined, with the first value being termed the ideal capacity and being calculated using the mean tensile strength of ECC (3.1 MPa) and a strength reduction factor (ϕ) of 1.00, and the second value being termed the design capacity and calculated using the design tensile strength of the ECC material (1.9 MPa) and a strength reduction factor of ϕ = 0.85 (phi only applied when ECC is acting as a tensile element) as is typically used in New Zealand reinforced concrete masonry flexural design [36]. When presenting the predicted capacities in the subsequent calculations, the bracketed values represent calculations based on the ECC design strength with a ϕ factor of 0.85 and the non-bracketed values represent calculations based on the ECC mean strength (or a steel bar mean strength of 340 MPa) with a ϕ factor of 1.00. For walls that were strengthened by amateur applicators

(W4-S25-C and W5-S30-C-NSM), the previously mentioned skill-based strength reduction factor (ϕ_s) of 0.75 was also applied to both the ideal and design capacity.

$$F_{total} = F_{RM} + F_{ECC} \tag{2}$$

$$F_{ECC} = \frac{8f'_{yECC}Z}{h} \tag{3}$$

The mechanism used to determine the cracked total lateral capacity (F_{RM}) of W1-S30-M-CL is similar to that used to predict the post-cracking capacity of unreinforced walls, where the masonry wall is assumed to act as two rigid bodies separated by the crack. The moment resisted is related to the height of the primary flexural wall crack above the wall base, the overburden force, the wall selfweight, the depth of the mortar joints in compression at wall base, and the geometry of the ECC overlay section that is in compression at the wall crack location. The force balancing mechanism for this situation is shown in Figure 7. The tensile strength of the mortar joints was assumed to be zero, as recommended by [37]. Equations 4-6 were obtained from [35] with partial simplification due to the absence of any overburden force. W is the wall selfweight per unit length of the wall in kN/m, β is the ratio of wall crack height measured from the wall base to the overall wall height, and c_1 and a are the rectangular stress block coefficient and depth (in mm) respectively. f'_j is the mortar compressive strength when assessing the compression zone width at the wall base or is the ECC compressive strength when assessing the compression zone width at the wall crack location, as the ECC overlay is the element in compression at intermediate wall heights (assuming that the value of a does not exceed the ECC overlay thickness). The total lateral capacity using the two assumed f'_j values are equal to 6.0 kN (4.9 kN) when mortar failure was critical and 6.4 kN (5.3 kN) when failure of the ECC overlay was critical, with result indicating that these values are not significantly different.

$$F_{RM} = \frac{Wtl}{(\beta - \beta^2)h}\left[2(1-\beta)\left(1 - \frac{1 + c_1}{2}\frac{a}{t}\right)\right] \tag{4}$$

$$a = \frac{W}{0.85 f_j'}(1-\beta) \tag{5}$$

$$c_1 = \frac{1}{(1-\beta)} \tag{6}$$

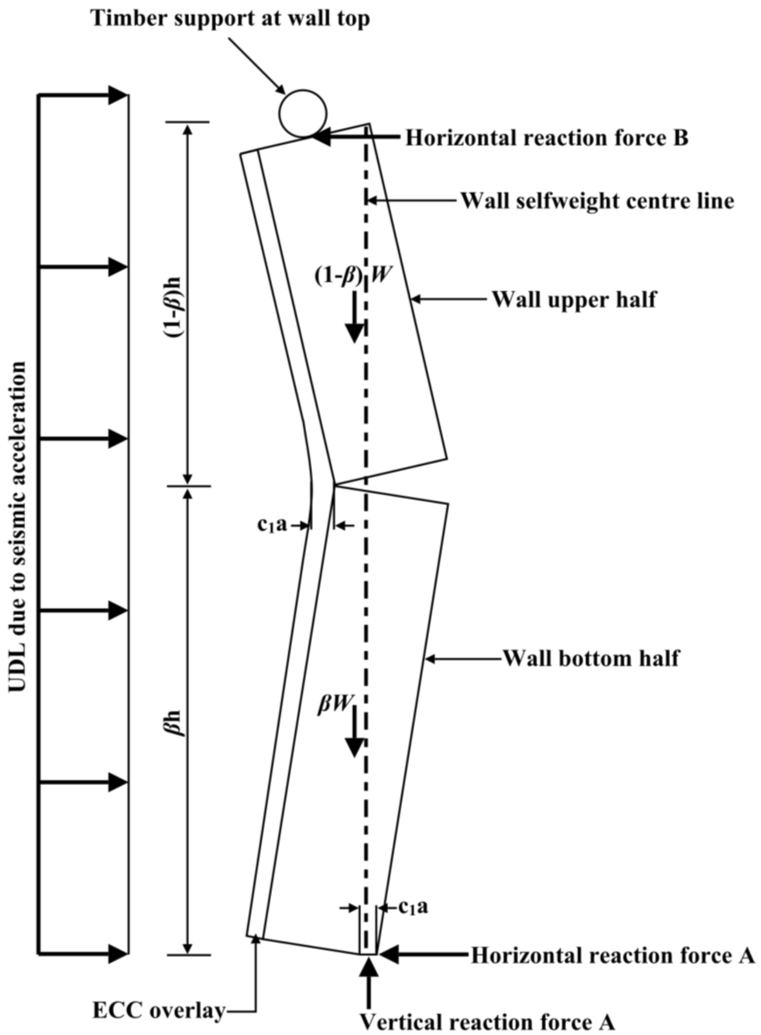

Figure 7: Schematic detailing the cracked wall selfweight balancing the lateral seismic forces

The measured load that was resisted by the wall was 7.4 kN, being 123% (151%) of the load calculated using Equation 2 and 170% of the average as-built wall strength, with this discrepancy likely arising from the assumed masonry density and the variability of the ECC thickness across the wall. This test result shows that application of an ECC overlay to the compression surface of the wall resulted in only a minor elevation in out-of-plane wall capacity, and while this improvement may be sufficient for areas of low seismicity, additional reinforcement will likely be required in most moderate and high seismicity scenarios. Attempts to further refine the accuracy of Equations 4-6 were deemed unnecessary as it is unlikely that the strength increase provided by the ECC overlay on the compression surface of the wall will be adequate if a URM building needs seismic intervention.

Wall W3-S30-M-TL had 30 mm of ECC shotcrete applied to the tensile surface of the wall and was loaded monotonically. The wall exhibited a brittle failure mode (see Figure 4d), with the load resisted increasing linearly until the ECC overlay cracked at wall mid-height, at which point the upper half of the wall displaced further than the lower half and collapsed. The moment capacity of the wall was calculated using a methodology identical to that used for reinforced concrete flexural design, where the masonry is treated as the compression member and the ECC overlay as the tension member. A 20 mm reduction in the masonry wall thickness was used as this was the largest depth that the mortar layers were typically set back from the brick wall surface. This reduction in thickness was also adopted in [22] when assessing the response of unstrengthened URM walls. A list of $\alpha f_m'$ values recommended by various publications [38-42] are provided in Table 5, where α is a factor that is used to convert the peak flexural compression stress to an equivalent uniform compression stress (α = 0.85 adopted in this study), and f_m' is the masonry compression strength. The moment capacity of the wall was calculated using Equations 7-10 incorporating the above variables and the material properties listed in Table 2. The tensile force (T) that can be resisted by the ECC overlay section was calculated to be 107.0 kN (65.6 kN) (Equation 7), with the axial load (N) due to the weight of the upper half of the wall being 9.3 kN. Using Equation 8, the total compressive force (C) was 116.3 kN (74.9 kN), which results in a compression zone width (a) calculated using Equation 9 of 20.0 mm (12.9 mm), where α was taken as 0.85 and f'_m and l are the masonry compressive strength and wall length respectively.

$$T = f'_{yECC} \times ECC\ cross\ sectional\ area \tag{7}$$

$$C = T + N \tag{8}$$

$$a = \frac{C}{\alpha f'_m \times l} \tag{9}$$

Table 5: List of $\alpha f'_m$ values recommended by different publications

$\alpha f'_m$	Publications	References
$0.86f'_m$	Designs of Structures for Earthquake Resistance Part 3: Assessment and Retrofitting of Buildings, Eurocode 8	[38]
$0.855f'_m$	Design Guideline for the Strengthening of Unreinforced Masonry Structures Using Fibre Reinforced Polymers (FRP) Systems	[39]
$0.85f'_m$	Masonry: Design on the Basis of Semi-Probabilistic Safety Concept, Din 1053-100	[40]
$0.80f'_m$	Building Code Requirement for Masonry Structures	[41]
$0.70f'_m$	Prestandard and Commentary for the Seismic Rehabilitation of Buildings	[42]

By balancing the moment calculated about the centroid location of the wall axial load (Equation 10), where t_{ECC} is the thickness of the ECC section, the moment capacity (M_n) of the wall was calculated as 23.9 kNm (12.9 kNm). Assuming the load to be uniformly distributed along the wall surface, the total lateral capacity of the wall (F_{ln}) calculated using Equation 11 was 46.6 kN (25.3 kN). The measured total lateral force on the wall was equal to 55.1 kN, being 118% (218%) of the predicted ideal (design) load and 1267% of the average as-built wall strength.

$$M_n = T \times \frac{t_{ECC} + t}{2} + C \times \frac{t - a}{2} \tag{10}$$

$$F_{ln} = \frac{8\phi M_n}{l} \tag{11}$$

Wall W4-S25-C had 25 mm of ECC overlay applied on a single surface of the wall and was loaded cyclically, with the load applied such that the ECC overlay was subjected to alternating tensile and compression stresses. The specimen was first loaded such that the ECC layer was located on the compression surface, up to a wall mid-height lateral displacement of 50 mm. The plywood frame and instrumentation setup was then shifted to allow the load to be applied such that the ECC overlay was located on the tensile surface of the wall. The load was applied to the wall up to a value of approximately 15 kN and then the air pressure was released, completing the first cycle of the test. After the first cycle, the wall was again loaded with the ECC overlay located on the compression surface up to a wall mid-height displacement of 70 mm. Finally the wall was loaded with the ECC overlay located on the tensile surface until the ECC overlay cracked at a total lateral load of 28.1 kN (see Figure 7e). The measured load was 138% (159%) and 96% (177%) of the predicted load when ECC was acting on the compression and tensile surface of loading respectively, with the strength increase being 344% and 645% of the average as-built wall strength

Wall W5-S30-C-NSM was strengthened using both a NSM reinforcing bar and 30 mm of ECC overlay, with the overall configuration detailed in Figure 2 and explained previously. For this design philosophy, when the wall is loaded with the ECC overlay located on the compression surface, the steel reinforcement will provide the tensile capacity needed to resist out-of-plane lateral loads, analogous to the concept used when designing a reinforced concrete T-beam.

The lateral capacity of W5-S30-C-NSM was calculated using concrete flexural design methodology, ignoring the tensile strength of the masonry but including the wall selfweight acting through the wall centreline. The ultimate tensile force (T) was equal to the reinforcing bar cross-section area multiplied by its tensile yield strength, and the compressive force (C) was calculated using Equation 8. The compressive force (C) was substituted into Equation 12 to determine the compression zone width (a), where f'_{ECC} is the compressive strength of ECC and l_{eff} is the effective flange width of the ECC section incorporating NSM steel reinforcement (see Figure 8), which is determined from the smallest of:

- The ECC web width (w_s) plus twice the steel embedment depth from ECC surface: $\left(w_s + 2(d_s + t_{ECC})\right) = 210\ mm$
- The ECC web width plus 16 times the ECC thickness applied over the wall surface: $(w_s + 16t_{ECC}) = 530\ mm$
- The ECC web width plus a quarter of the wall height: $\left(w_s + \frac{h}{4}\right) = 1075\ mm$
- The centre to centre spacing between NSM bars: $\mathrm{S} = 1150\ mm$

The compressive zone width *a* determined using Equation 12 was 14.9 mm, being within the ECC flange thickness of 30 mm, and x_c, the distance from the extreme compressive fibre to the centroid of the compressive force was 7.5 mm (Equation 13) from the ECC overlay surface. If the compressive force (C) exceeds the compressive capacity of the ECC flange section ($\alpha \times f'_{ECC} \times l_{eff} \times t_{ECC}$) then Equation 14 and 15 should be used to determine the dimension of x_c.

For $C \le \alpha \times f'_{ECC} \times l_{eff} \times t_{ECC}$

$$a = \frac{C}{\alpha f'_{ECC} \times l_{eff}} \tag{12}$$

and

$$x_c = \frac{a}{2} \tag{13}$$

For $C > \alpha \times f'_{ECC} \times l_{eff} \times t_{ECC}$

$$a = \frac{(C - \alpha f'_{ECC} \times l_{eff} \times t_{ECC})}{\alpha f'_{ECC} \times w_s} \tag{14}$$

and

$$x_c = \frac{\left(\alpha f'_{ECC} \times l_{eff} \times t_{ECC} \times \frac{t_{ECC}}{2}\right) + \left(\alpha f'_{ECC} \times l_{eff} \times w_s \times \left(t_{ECC} + \frac{a}{2}\right)\right)}{C} \tag{15}$$

The moment capacity (M_n) of W5-S30-C-NSM was determined using Equation 16, after checking that the depth of the steel reinforcement (d_s) did not exceed the depth to the masonry wall centre line and that forces are considered about the line of action of the axial load (see Figure 8). The moment capacity of the wall was converted to the predicted lateral capacity using Equation 11 and was shown to be 8.5 kN (11.2 kN) when the ECC overlay was applied on the compression surface of loading. The predicted lateral resistance of the wall when the ECC overlay was acting on the tensile surface of loading was 35.0 kN (19.0 kN).

$$M_n = C \times \left(\frac{t}{2} + t_{ECC} - x_c\right) - T \times \left(\frac{t}{2} - d_s\right) \tag{16}$$

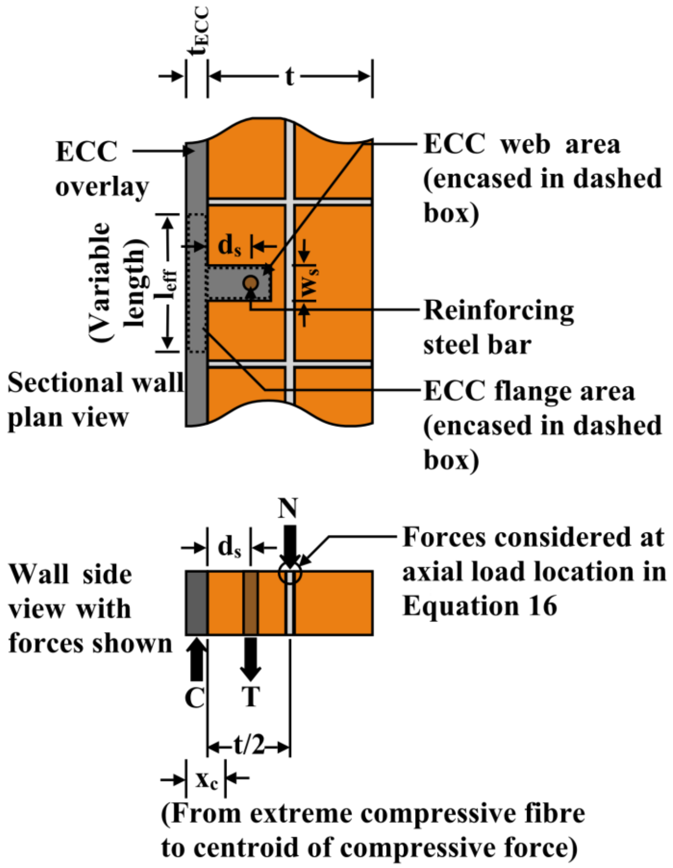

Figure 8: Schematics detailing the variables used to determine the moment capacity in Equation 16 and the balancing of forces

W5-S30-C-NSM was initially loaded cyclically five times in one direction with increased displacement between each cycle, with the ECC overlay located on the wall compression surface. During the fifth cycle, loads were applied until the peak strength of 14.6 kN (336% of the average as-built wall strength) was reached and the steel reinforcing bar debonded, as further described below. The test setup was then shifted to the opposite wall surface and the wall was loaded for eight cycles with the ECC overlay located on the tensile surface, with an increased load applied between each cycle and a peak load of 36.6 kN obtained during the eighth cycle (see Figure 4f). The direction of loading did not alternate between wall surfaces for each cycle, so that the maximum moment capacity for the case when the ECC overlay was on the compression surface of the wall was determined without risk of premature wall failure arising from the ECC overlay being loaded in tension during reversed cycling. Determining the maximum load that was developed when the ECC overlay was acting on the tensile wall surface was not a priority as similar data was already available from the testing of specimens W3-S30-M-TL and W4-S25-C. The maximum total lateral load measured when the ECC overlay was located on the tensile surface was 36.6 kN, being 105% (193%) of the predicted load and 841% of the average as-built wall strength.

Post-test examination of wall W5-S30-C-NSM showed that the steel reinforcing bar did not rupture, but instead debonded from the ECC shotcrete over a length of approximately 1.0 m when measured from the wall top. The debonding was caused by incomplete encasement of the steel reinforcing bar at the particular location. The bond behaviour of steel reinforcing bar to the surrounding ECC matrix and the ECC matrix to the surrounding masonry elements is a subject that requires additional experimental confirmation, particularly with regards to the consistency achieved in field applications. However, this is beyond the scope of the current study. Despite the debonding failure mode exhibited, the capacity of W3-S30-M-TL exceeded the predicted capacity, demonstrating that the wall satisfactorily achieved the capacity determined using concrete flexural design methodology. In practical application, it may be possible to epoxy the bottom end of the steel reinforcing bar into the building foundation and have the top end connected to an anchor plate at wall top to mitigate the potential for debonding.

Comparison with alternative strengthening techniques

Table 6 provides an overall summary comparison with experimental results obtained through alternative strengthening techniques where the test setup, specimen dimension and masonry material properties are similar [10, 24]. The lower bound maximum lateral load is similar across all three strengthening techniques, while the upper bound value is significantly higher for ECC than the alternative options. However, the comparisons were made for the investigated retrofit configuration only, as alternative retrofit configurations such as thinner ECC layers or additional CFRP strips may well yield alternative results. A cost comparison was not adopted as the selection of strengthening techniques is often governed by existing building layout and heritage restrictions and the cost of implementation can be highly variable depending on the aforementioned factors.

Table 6: Comparison with alternative strengthening techniques with similar test setup

Strengthening techniques	Application surface	Retrofit configuration	Measured maximum lateral loads (kN)
ECC	Single	Refer to main text for configuration	14.6-55.1
NSM CFRP	Single	Installation of one to two 15 mm wide CFRP strip vertically down the wall, embedded 20 mm into the wall face. Tested with CFRP on the tension face only.	14.3-33.9
Post-tensioning	Internal	Post-tensioned using either threaded steel bar or strand, post-tension stress varies between 442 MPa-1013 MPa	13.2-29.8

Design methodology

Based on the results obtained in this study, the following design methodology is proposed for out-of-plane strengthening of URM walls using ECC shotcrete or other similar fibre reinforced cement composites. It should be noted that the proposed design methodology was verified using the assumptions and boundary conditions stated in this study, such that adaptation of this design methodology for deviated scenarios requires further verification.

1. Determine the required design moment capacity based upon seismicity of the site and an appropriate local design guide such as [43], and establish the axial load based on material density and any overburden. Check the existing wall strength using Equation 1, and proceed with strengthening design if required.
2. If ECC is to be applied on a single surface of the wall then the critical case is typically when the ECC overlay is acting on the compression surface of the wall. The out-of-plane strength of a wall with an ECC overlay only can be calculated using Equations 2-6.
3. If the capacity calculated above is not sufficient with an ECC overlay only then near surface mounted steel reinforcing bars will be required to resist the lateral load. Make initial assumptions on the required reinforcing bar diameter, spacing and embedment depth, and consequently determine the ECC web width and depth based on the required reinforcement cover. Adjust the design moment (M^*) depending on the NSM reinforcing bar spacing so that only a section of the wall is considered.
4. Using the assumed steel bar diameter and steel tensile strength, determine the compressive force (C) using Equation 8, where T and N are the tensile forces that can be resisted by the reinforcing bar and the axial force imposed on the wall (inclusive of wall upper half selfweight) respectively. Calculate the width of the compressive zone and the distance to the centroid of the compressive force using Equations 12 and 13. If the compression zone width (a) exceeds the thickness of the ECC flange section (t_{ECC}), then Equations 14 and 15 should instead be used to calculate the centroid of the compression zone.

5. Determine the moment capacity (M_n) according to Equation 16, assuming that the depth of the steel reinforcement does not exceed the masonry wall centre line and that forces are considered about the line of action of the axial load.
6. If no anchorage plates are used at reinforcing bar ends, check the bond between the steel reinforcement bar and the surrounding ECC shotcrete using an appropriate equation. Alternatively, a pre-application test can be conducted to assess the peak bond strength that can be achieved based upon the competency of the shotcrete applicator.
7. Check the moment capacity of the wall when the ECC overlay is acting on the tensile surface, treating the masonry as the compression member and ECC as the tensile member using Equations 7-10 and check that $\phi \times \phi_s M_n \geq M^*$, where M^* is the design moment, ϕ_s is the skill strength reduction factor, equal to 1.00 when the shotcrete is applied by professional applicators and equal to 0.75 for amateur applicators and ϕ is the strength reduction factor, equal to 0.85. If the capacity is not sufficient, increase the ECC overlay thickness or re-design the steel reinforcement detail.
8. If ECC shotcrete is to be applied on both surfaces of the wall (such as on internal walls), assume an equal thickness of ECC on both surfaces and assume that one ECC overlay is the tensile element and that the other ECC overlay is the compressive element. Calculate the tensile force (T) based on the ECC tensile strength × the ECC cross-sectional area (on one surface). Determine the axial force (N) of the masonry wall based on wall geometry and density (and any overburden forces) and calculate the compressive force C according to Equation 8. Calculate the width of the ECC

compressive zone (a) using Equation 21, where f'_{ECC} is the compressive strength of ECC and all other variables are identical to those used in Equation 9.

$$a = \frac{C}{\alpha f'_{ECC} \times l} \tag{21}$$

9. Determine the moment capacity by considering the forces about the point of axial load using Equation 10, and check that $\phi \times \phi_s M_n \geq M^*$. If the capacity is insufficient, increase the total ECC thickness.

Conclusion

This study investigated the effectiveness of ECC shotcrete and near surface mounted (NSM) steel reinforcing bars as URM wall strengthening technique for out-of-plane lateral loads. Five masonry walls were constructed and a total of six tests were conducted using either monotonic or cyclic lateral loads. A design procedure was presented and the following conclusions can be made:

1. As-built unreinforced clay brick masonry walls with an assumed pinned support at both wall top and bottom have a weak out-of-plane moment capacity and the wall cracking strength was able to be predicted using existing equations.
2. When 30 mm of ECC overlay was applied onto the compression surface of the URM wall, the strength of the wall increased by 170% when compared to the average strength of the two as-built URM walls. The retrofitted wall strength was equal to the combined capacity of the ECC overlay flexural strength and the lateral load that can

be resisted by the selfweight of the wall, assuming that the wall breaks into two separate rigid bodies.

3. When ECC overlay was applied to the tensile surface of the wall, wall strength increased between 646%-1267% when compared to the out-of-plane strength of the as-built URM walls. The strength of a wall having an ECC overlay can be determined using methods analogous to concrete flexural design, treating the ECC overlay as the tensile resisting member and the masonry as the compression member.
4. When a grade 300 MPa D20 deformed reinforcing bar was embedded 50 mm from the masonry wall surface, the strength of the wall with the ECC overlay acting on the compression surface increased by 336%, The strength of the section exceeded the value determined using concrete flexural design. Additional investigation into the bond strength between the ECC overlay and the embedded reinforcement is required.
5. ECC strengthened URM wall capacities for scenarios and boundary conditions similar to those adopted in this study can be determined using existing design methodologies. When ECC overlay is only applied on one surface of a URM wall, the use of NSM steel reinforcement is recommended. Adaption of the proposed design methodology for cases differing from those reported herein will require further verification.
6. Overall it was shown that the application of ECC shotcrete is a feasible approach for the seismic strengthening of unreinforced masonry walls. Further investigation of the bond behaviour between steel reinforcement and ECC is recommended to establish more refined predictive equations.

Acknowledgements

The authors wish to acknowledge Bing Zhang, Karl Yuan and Anthony Le Dain for their assistance in sample production, preparation and testing. The authors also thank David Nevans, Michael Barry and Roydon Gilmour from Reid Construction Systems for providing the equipment required for this study. Lastly, the authors thank the New Zealand Ministry of Science and Innovation for the funding of Dr Lin's doctoral study and the New Zealand Earthquake Commission for the funding of Dr. Wotherspoon's position at the University of Auckland.

References

1. NZS (1965). "Model building bylaw." NZS 1900:1965, New Zealand Standards Institute. Wellington, New Zealand.

2. Russell, A. P. and Ingham, J. M. (2010). "Prevalence of New Zealand's unreinforced masonry buildings." *Bulletin of the New Zealand National Society for Earthquake Engineering*, 43(3): 182-202.

3. Goodwin, C. P. (2009). "Architectural considerations in the seismic retrofit of unreinforced masonry heritage buildings in New Zealand." School of Architecture and Planning, University of Auckland. Auckland, New Zealand. M.Arch: 215.

4. Lam, N. T. K., Griffith, M., Wilson, J. and Doherty, K. (2003). "Time-history analysis of URM walls in out-of-plane flexure." *Engineering Structures*, 25(6): 743-754.

5. Griffith, M. C., Magenes, G., Melis, G. and Picchi, L. (2003) "Evaluation of out-of-plane stability of unreinforced masonry walls subjected to seismic excitation." *Journal of Earthquake Engineering*, 7(Special issue 1):141-169.

6. Sharif, I. Meisl, C. S., and Elwood, K. J. (2007). "Assessment of ASCE 41 height-to-thickness ratio limits for URM walls." *Earthquake Spectra*, 23(4): 893-908.

7. McDowell, E., Mckee, K. J. and Ventura, C. E. (1956). "Arching action theory of masonry walls." Journal of Structural Division, 82(2): 1-18.

8. Moon, L., Dizhur, D. Senaldi, I., Derakhshan, H., Griffith, M., Magenes, G. and Ingham, J. M. (2014) "The demise of the URM building stock in Christchurch during the 2010/2011 Canterbury earthquake sequence." *Earthquake Spectra*, 30(1): 253-276.

9. Gilstrap, J. M. and Dolan, C. W. (1998). "Out-of-plane bending of FRP-reinforced masonry walls." *Composites Science and Technology,* 58(8): 1277-1284.

10. Dizhur, D., Griffith, M. C., and Ingham, J. M. "Out-of-plane strengthening of unreinforced masonry walls using near surface mounted fibre reinforced polymer strips." *Engineering Structures*, 59:330-343.

11. Galati, N., Tumialan, G. and Nanni, A. (2006). "Strengthening with FRP bars of URM walls subject to out-of-plane loads." *Construction and Building Materials*, 20: 101-110.

12. Papanicolaou, C., Triantafillou, T., Papathanasiou, M. and Karlos, K. (2008). "Textile reinforced mortar (TRM) versus FRP as strengthening material of URM walls: out-of-plane cyclic loading." *Materials and Structures,* 41(1): 143-157.

13. Liang, C. and Y. Che (2011). "Seismic analysis of multilayer masonry structure strengthened with shotcrete using RVE." *Earthquake Resistant Engineering and Retrofitting*, 33(6): 12-18.

14. Kanda, T., Saito, T., Sakata, N. and Hiraishi, M. (2003). "Tensile and anti-spalling properties of direct sprayed ECC." *Journal of Advanced Concrete*, 1(3): 269-282.

15. Maalej, M., Lin, V. W. J., Nguyen, M. P. and Quek, S. T. (2010). "Engineered cementitious composites for effective strengthening of unreinforced masonry walls." *Engineering Structures*, 32(8): 2432-2439.

16. Rokugo, K., Kunieda, M., Miyazato, S. and Konsta-Gdoutos, M. S. (2006). "Structural applications of HPFRCC in Japan." *Proc., Measuring, Monitoring and Modelling Concrete Properties (MMMPC),* Springer Netherlands. Alexandroupolis, Greece. July 3-7. pg. 17-23.

17. Shin, S. K., Kim, J. J. H. and Lim, Y. M. (2007). "Investigation of the strengthening effect of DFRCC applied to plain concrete beams." *Cement and Concrete Composites*, 29(6): 465-473.

18. Lin, Y., Scott, A., Wotherspoon, L. and Ingham, J. M. (2014). "In-plane strengthening of unreinforced clay masonry wallettes using ECC shotcrete". *Engineering Structures:* 66: 57-65.

19. Bruedern, A-E., Abecasis, D. and Mechtcherine, V. (2008). “Strengthening of masonry using sprayed strain hardening cement-based composites (SHCC).” *7th RILEM Symposium on HPFRCC*. Chennai (Madras), India. September 17-19.Pg. 451-460.

20. Kesner, K and Billington, S. L. (2005). “Investigation of infill panels made from Engineered Cementitious Composites for seismic strengthening and retrofit.” *Journal of Structural Engineering*, 131(11).

21. Kyriakides, M. A., Billington, S. L., Shing, B. P., William, K. Stavridis, A and Blackard, B. (2009). “Evaluation of a sprayable, ductile cement-based composite for the seismic retrofit of unreinforced masonry infills.” *Improving the Seismic Performance of Existing Buildings and Other Structures*. San Francisco, California, United States. September 9-11. Pg. 823-834.

22. Derakhshan, H., (2011). “Seismic assessment of out-of-plane loaded unreinforced masonry walls.” Department of Civil and Environmental Engineering, University of Auckland, Auckland, New Zealand. PhD: 341.

23. Derakhshan, H., Griffith, M. and Ingham, J. M. (2013). “Airbag testing of multi-leaf unreinforced masonry walls subjected to one-way bending.” *Engineering Structures:* 57: 512-522.

24. Ismail, N., and Ingham, J. M. (2012). “Cyclic out-of-plane behaviour of slender clay brick masonry walls seismically strengthened using posttensioning”, *Journal of Structural Engineering*, 138(10), doi: 10.1061/(ASCE)ST.1943-541X.0000565

25. Dizhur, D., Derakhshan, H., Griffith, M. and Ingham, J. M. (2011). “In-situ testing of a low intervention NSM seismic strengthening technique for historic URM buildings.” *International Journal of Materials and Structural Integrity*: 5(2/3): 168-191.

26. Dizhur, D., Griffith, M. and Ingham, J. M. (2014). “Out-of-plane strengthening of unreinforced masonry walls using near surface mounted fibre reinforced polymer strips.” *Engineering Structures:* 59: 330-343.

27. Lin, Y., Derakhshan, H., Dizhur, D., Lumantarna, R., Wotherspoon, L. and Ingham J. M. (2011). “Testing and seismic retrofit of 1917 Wintec F block URM building in Hamilton.” *Structural Engineering Society (SESOC)*, 24(1): 47-57.

28. Derakhshan, H., Dizhur, D., Lumantarna, R. Cuthbert, J., Griffith, M. C. and Ingham, J. M. (2010). “In-field simulated seismic testing of as-built and retrofitted unreinforced masonry partition walls of the William Weir house in Wellington.” *Structural Engineering Society (SESOC)*, 23(1): 51-61.

29. ASTM-C67 (2001a). “Standard test methods for sampling and testing brick and structural clay tile.” ASTM-C67-00, Masonry test methods and specifications for the building industry, American Society for Testing and Materials. Virginia, USA.

30. ASTM-C-109/C-109M (2001b). “Standard test method for compressive strength of hydraulic cement mortars (using 2-in or 50-mm cube specimens).” ASTM-C-109/C-109M -99, Masonry test methods and specifications for the building industry, American Society for Testing and Materials. Virginia, USA.

31. ASTM-C-1314 (2001c). “Standard test method for compressive strength of masonry prisms.” ASTM-C-1314-00a, Masonry test methods and specifications for the building industry, American Society for Testing and Materials. Virginia, USA.

32. Russell, A. P. (2010) “In-plane seismic assessment of unreinforced masonry buildings.” Department of Civil and Environmental Engineering, University of Auckland. Auckland, New Zealand. PhD: 312.

33. ASTM-E-72 (2010). “Standard test methods of conducting strength tests of panels for building construction.” ASTM-E-72, American Society for Testing and Materials. Philadelphia, USA.

34. Lin, Y., Biggs, D., Wotherspoon, L. and Ingham, J. M. (2012) “In-plane strengthening of unreinforced concrete masonry wallette using ECC shotcrete mix.” *Journal of Structural Engineering:* 1-13. doi: 10.1061/(ASCE)ST.1943-541X.0001004

35. Derakhshan, H., Griffith, M. C. and Ingham, J. M. (2012). “Out-of-plane behavior of one-way spanning unreinforced masonry walls.” *Journal of Engineering Mechanics*, 139(4): 409-417. doi: 10.1061/(ASCE)EM.1943-7889.0000347

36. NZS (2004). “Design of reinforced concrete masonry structures.” NZS 4230:2004, Standards New Zealand. Wellington, NZ.

37. ASCE (2007). “Seismic rehabilitation of existing buildings.” ASCE/SEI Standard 41, Structural Engineering Institute. American Society of Civil Engineers. Reston, Virginia, USA.

38. CEN (2005). “Designs of structures for earthquake resistance part 3: assessment and retrofitting of buildings.” Eurocode 8, European Committee for Standardization. Brussels, Belgium.

39. Galati, N., Garbin, E. and Nanni, A. (2005). “Design guideline for the strengthening of unreinforced masonry structures using fibre reinforced polymer (FRP) systems.” University of Missouri-Rolla, Missouri, USA.

40. DIN (2004). “Masonry: design on the basis of semi-probabilistic safety concept.” DIN 1053-100, Germany Institute for Standardization. Berlin, Germany.

41. MSJC (2002). “Building code requirement for masonry structures.” ACI 530-04/ASCE 5-04/TMS 402-04, Masonry Standards Joint Committee. Boulder, Colorado, USA.

42. BSCC (2000). “Prestandard and commentary for the seismic rehabilitation of buildings.” FEMA 356, Building Society Safety Council. Washington, USA.

43. NZS (2004). “Structural design actions part 5: earthquake actions - New Zealand.” NZS 1170.5:2004, New Zealand Standards Institute. Wellington, New Zealand.